Robustly Stabilizing Individual Generators with Gain-scheduling SVC via the Small-gain Theorem

Jun Zhou*, Qiufang Zhang

Department of Automatic Control Engineering, School of Energy and Electrical Engineering, Hohai University

Xikang Rd 1, Nanjing 210098, Jiangsu, China

*1katsura@hhu.edu.cn 2 hisashimax178@sina.com

Abstract

Individual generators in multi-machine networks are represented by closed-loop configurations of linear time-invariant modeling and nonlinear feedback, subject to modeling uncertainties and power disturbances, based on which control laws and implementation algorithms of static VAR compensators (SVC) are established to robustly stabilize individual generators by combining the gain-scheduling technique to the small-gain theorem in the sense of finite-gain L_2 -stability. The gain-scheduling SVC manipulation approach can be implemented in multiple decentralized algorithms that involve only locally-measured signals, and are robust against modeling uncertainties and power disturbances. The suggested SVC control laws can also accommodate the steady-state performance specification in term of generator power angle, besides stabilization. As a special case of the suggested SVC control laws, examples are included to illustrate efficacy and simplicity of an averagely gain-scheduling SVC control law.

Keywords

Swing Equation; Static VAR Compensator; Gain Scheduling; Small-gain Theorem; Finite-gain L_2 *-stability*

Introduction

Stabilization of individual synchronous generators in multi-machine power networks is inevitable and of engineering significance much higher than most techniques for stabilizing all generators [Alberto & Bretas, Cong et al., Gupta et al., Yang et al.] simultaneously, which usually involve complicated control laws and expensive communication devices, and high maintenance cost, though some of them are implementable in decentralized ways [Aboul-Ela et al., Damm et al., Fan & Feliachi, Lu et al., Wang et al., J. Zhou (2010a)]. Stabilization problems in synchronous generators are also conventionally formulated as power swing reduction, to which numerous papers are devoted in miscellaneous stability meanings, and latest results are reported in [Chiang & Chu, Haque (2005), Liu et al., Salam et al., J. Zhou & Ohsawa, J. Zhou (2010b)].

Robustly stabilizing individual generators in a multi-machine network in the finite-gain L_2 -stability via flexible ac transmission systems (FACTS) [Haque (2004), Lerch et al.] is considered in the study. Control laws of static VAR compensators (SVC) are developed by exploiting the gain-scheduling mechanism [H. K. Khalil(2002)] and the small-gain theorem [Vidyasagar]. The gain-scheduling SVC approach possesses many advantages, for example, it can be implemented in multiple decentralized fashions that involve only locally measured feedback signal (and thus, no time-delay concerns in power networks need to be taken into account); and it can cope with power disturbances and modeling uncertainties such as those in damping windings, and results in robust stabilization for us. An implementation algorithm for the suggested SVC control law is also contrived, which can also accommodate the steady-state power angle specification, besides stabilization. However, our numeric simulations show that the suggested SVC control laws may be conservative, compared to those of [J. Zhou (2010b)].

By the literature, neither damping windings nor disturbances can be dealt with accurately and effectively by the equal area criterion (EAC) [Haque (2004, 2005), E. Z. Zhou]. EAC is a graphical tool, and requires expertise operators with expertise. Lyapunov theory is also frequently employed for stabilizing generators, which usually yields sophisticated nonlinear algorithms with high conservatism [Yang, J. Zhou (2010a)]. Recently, pole assignment and least quadratic regulation are adopted for SVC control law

design [J. Zhou (2010b)], whose engineering efficacy depends closely on modeling, measuring devices and actuators.

The second section collects facts on swing equations of individual generators with SVC's connected, their state-space re-expression and feedback configuration interpretation; and stabilization problem is formulated as well in the section. The third section introduces concepts and useful stability criteria. The next section talks about stabilization control laws of SVC's by combining the gain-scheduling technique and the small-gain stability theorem. The third and fourth sections are the main context. Illustrative examples are sketched in the fifth section with an implementation algorithm of the average gain-scheduling SVC control law, while the final section states our conclusions.

Preliminaries and Problem Formulation

Individual Generator Systems and Equivalent Swing Equations

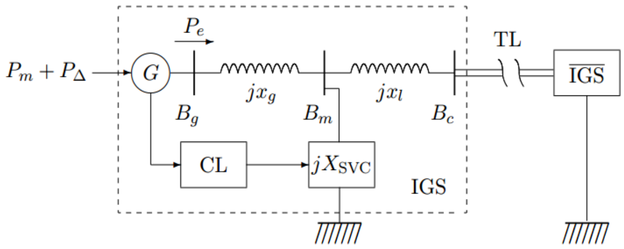

FIG. 1 IGS CONFIGURATION IN A MULTI-MACHINE NETWORK

An individual generator system (IGS) is isolated from the multi-machine network as in Figure 1, where $\overline{\text{IGS}}$ represents the remaining multi-machine portion connected with the IGS via the transmission line (TL). B_g, B_m and B_c, respectively, are the internal bus, the terminal bus to which a shunt SVC is connected, and the local load bus to which TL is linked. x_g is the reactance between B_m and B_g, while x_l is that between B_m and B_c. SVC is parameterized as variable reactance X_{SVC} as in [Haque (2004, 2005)]. P_m is the mechanical power from turbine and governor, and P_e is the electrical power viewed at B_g. CL represents the control law that manipulates the SVC.

Based on [Haque (2005)] and the re-modeling technique of [J. Zhou (2010b)], an equivalent swing equation depicting the dynamics of the generator rotor with a shunt SVC as in Figure 1 is

$$\Sigma:\begin{cases}\dot{\delta}=\omega\\ \dot{\omega}=-\dfrac{D}{J}\omega-\dfrac{b\sin\delta}{xM}+\dfrac{P_m+P_\Delta}{M}\end{cases}\tag{1}$$

where $b = E_c E_g$ and $x = x_g + x_l - X_{SVC} x_g x_l$ with E_c and E_g are the virtual voltages of B_c and B_g, respectively. Voltage deviations from E_c and E_g are reflected by perturbation in P_m. Complicated but weak dynamics of the SVC are viewed as uncertainties and added to P_Δ. It is hard to handle P_Δ exactly. It is assumed that P_Δ is a bounded disturbance.

Also in (1), δ and ω are the generator rotor angular displacement and velocity, respectively, with respect to a reference axis on B_c rotating at the system angular frequency ω_s [Kimbark]; J: combined inertia moment of the generator rotor (kg·m²); and $M = J\omega_s$; D: mechanical and electrical damping due to amortisseur windings [Anderson & Fouad, Machowski et al.].

State-Space Expression of IGS and Closed-Loop Configuration

In what follows, let δ be the output of the IGS, that is, $y=\delta$. In the steady state, δ is called the power angle of the generator, which is related to the power factor that reflects the power generation efficiency of the generator. Based on (1), the IGS is described by the state-space representation

$$\Sigma:\begin{cases}\dot{\varsigma}=A\varsigma+B(P_m+P_\Delta)+\begin{bmatrix}0\\-b\sin\delta/M\end{bmatrix}x^{-1}\\ y=C\varsigma\end{cases}\tag{2}$$

where $\varsigma := [\delta,\omega]^T$ and

$$A=\begin{bmatrix}0, & 1\\ 0, & -D/J\end{bmatrix}, B=\begin{bmatrix}0\\1/M\end{bmatrix}, C=[1,0]$$

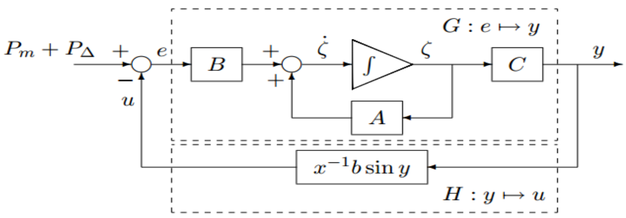

FIG. 2 FEEDBACK CONFIGURATION INTERPRETATION FOR THE IGS

Examining (2) carefully reveals readily that it is essentially nonlinear, and possesses a feedback configuration interpretation of Figure 2. Now we briefly denote

$$\begin{cases} G(s) = C(sI_2 - A)^{-1}B = [Ms(s + D/J)]^{-1} \\ H(x, y) = x^{-1}b\sin y \end{cases} \quad (3)$$

It is self-evident that $G(s)$ is the transfer function of the LTI subsystem $G: e \mapsto y$ and $H(x, y)$ is a nonlinear function reflecting the mapping $H: y \mapsto u$.

Finite-Gain L2-Stabilization Problem Formulation

Denote the Hilbert functions linear space $L_2 =: \{x(t) \in R^n | (\int_0^\infty \|x(\tau)\|^2 d\tau)^{1/2} < \infty$. Finite-gain L_2-stability definition and the small-gain theorem can be found in [Khalil, Vidyasagar]. Under the configuration of Figure 2, the small-gain theorem [Khalil, p. 218] provides us with a sufficient condition for the closed-loop system to be finite-gain L_2-stable as follows.

$$\|G\|_{L2/L2} \cdot \|H\|_{L2/L2} < 1 \quad (4)$$

where $\|\cdot\|_{L2/L2}$ is the L_2-induced norm of $(\cdot)$ Stabilization in finite-gain L_2-stability of the IGS is formulated as follows: determine SVC reactance manipulating laws such that (4) is satisfied.

Gain-Scheduling Small-Gain Theorem Interpretation

Loop Transformation

One might suggest that we use the H_∞ norm of $G(s)$ in place of $\|G\|_{L_2/L_2}$ in (4). We have

$$\|G\|_{L2/L2} = \|G\|_\infty := \sup_{\varphi\in(-\infty,\infty)} \|G(j\varphi)\|_2 \\ = \sup_{\varphi\in(-\infty,\infty)} |G(j\varphi)|.$$

However, $G(s)$ possesses a pole at the origin, and thus $\|G\|_\infty = \infty$. This hampers us from exploiting the small-gain inequality (4) directly in determining control laws to SVC.

To surmount $\|G\|_\infty = \infty$, a loop transformation K is introduced to the configuration of Figure 2 as in Figure 3. The input/output relationships in Figure 2 and 3 are the same. It is clear that

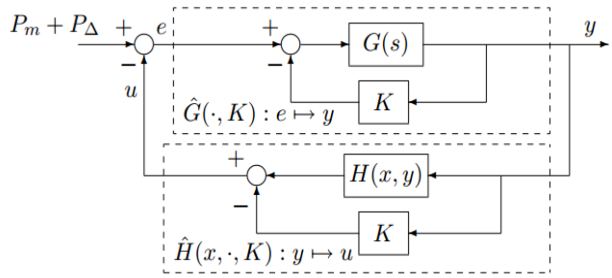

FIG. 3 LOOP TRANSFORMATION IN THE IGS CONFIGURATION

$$\begin{cases} \hat{G}(s, K) =: \dfrac{G(s)}{1 + KG(s)} = \dfrac{1}{Ms(s + D/J) + K} \\ u = H(x, y) - Ky = (\dfrac{b\sin y}{y} x^{-1} - K)y \\ = (\theta(y)x^{-1} - K)y := \hat{H}(x, y, K)y \end{cases} \quad (5)$$

where $\theta(y) = b\sin y / y$. The LTI subsystem $\hat{G}(s, K)$ is stable as long as $K > 0$.

Under the configuration of Figure 3, the small-gain inequality is

$$\|\hat{G}(\cdot, K)\|_{L2/L2} \cdot \|\hat{H}(x, \cdot, K)\|_{L2/L2} < 1 \quad (6)$$

Apparently, $\|\hat{G}(\cdot, K)\|_{L2/L2}$ is equal to the H_∞ norm of $\hat{G}(s, K)$, namely $\|\hat{G}(\cdot, K)\|_\infty$, which can be given numerically via the bi-section algorithm [K. Zhou & Doyle]. A closed-form expression for $\|\hat{G}(\cdot, K)\|_\infty$ is available in Appendix A. However, $\|\hat{H}(x, \cdot, K)\|_{L2/L2}$ cannot be given explicitly due to its obvious nonlinear feature.

Gain-Scheduling According to Phase Plane Partitioning

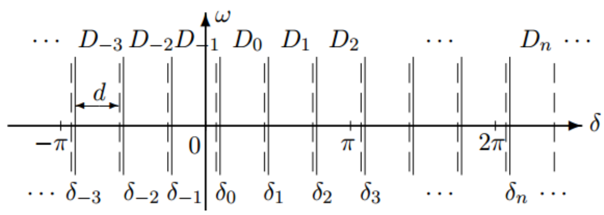

FIG. 4 PHASE PLANE PARTITIONING

To reduce conservatism of the small-gain inequality (6), $\|\hat{G}(\cdot, K)\|_{L_2/L_2}$ and $\|\hat{H}(x, \cdot, K)\|_{L_2/L_2}$ should be estimated as accurately as possible. To this end, the gain-scheduling technique is employed [Khalil]. We firstly partition the phase plane of (2) as in Figure 4, in which the solid lines are the left (included) boundaries

for D_i and the dashed lines are their right (not included) boundaries; namely $D_i =: \{(\delta, \omega) \in R^2 : \delta_i \le \delta < \delta_{i+1}\}$. The sub-regions are sufficiently sufficient so that $\bigcup_i D_i$ contains all phase portraits of (2) that interest us, while each D_i is narrow enough (or d is sufficiently small) so that $\delta \doteq \delta_i$ is reasonable for every $\delta \in D_i$.

According to the phase plane partitioning, it is assumed that for all $\delta = y \in D_i$,

$$\begin{cases} \hat{G}(\cdot, K) = \hat{G}(\cdot, K_i) \\ \hat{H}(x, \cdot, K)y = [(\theta(\delta_i)x_i^{-1} - K_i) + \nabla_i]y \\ = [\hat{H}(x_i, \delta_i, K_i) + \nabla_i]y \end{cases}$$

where $K_i > 0$ is a loop transformation introduced for $\delta = y \in D_i$; namely the loop transformation of Figure 3 is replaced with a gain-scheduling one $\{\cdots, K_{-1}, K_0, K_1, \cdots\} =: K$ defined according to $\{\cdots, D_{-1}, D_0, D_1, \cdots\} =: D$. K_i is used as a design parameter over D_i. Correspondingly, x_i is the control action of the SVC for $\delta = y \in D_i$; namely, the control law of the SVC is also gain-schedulingly manipulated, denoted by $\{\cdots, x_{-1}, x_0, x_1, \cdots\} =: X$. In addition, ∇_i means the modelling mismatch when $\hat{H}(x, \cdot, K)$ is approximated with $\hat{H}(x_i, \delta_i, K_i)$; clearly, ∇_i depends on x_i and $\delta \in D_i$ but independent of K_i. In the following, all ∇_i are simply viewed as bounded modelling uncertainties and collectively denoted by $\nabla := \{\cdots, \nabla_{-1}, \nabla_0, \nabla_1, \cdots\}$; namely

$$\begin{cases} \lim_{d \to 0} |\nabla_i| = 0 \\ \sup\limits_{\forall \delta \in D_i} |\nabla_i| < c \end{cases} \tag{7}$$

for all i. In (7) d is the sub-region width defined in Figure 4, and $0 < c < \infty$ is a (small) constant.

With the gain-scheduling approach, Figure 3 is re-drawn as a gain-scheduling configuration of Figure 5. By the notations of Figure 5, the small-gain inequality (6) is modified as

$$\|G(\cdot, K)\|_{L2/L2} \cdot \sup_{\forall \nabla} \|H(X, \cdot, K) + \nabla\|_{L2/L2} < 1 \tag{8}$$

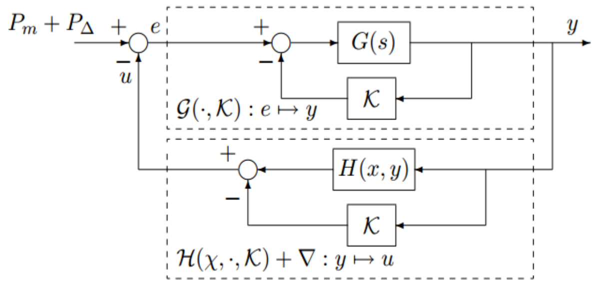

FIG. 5 GAIN-SCHEDULING LOOP TRANSFORMATION CONFIGURATION IN THE IGS

To exploit the gain-scheduling framework, we must answer: i) are $G(\cdot, K)$ and $H(X, \cdot, K) + \nabla$ meaningful as mappings on L_2? ii) can we get upper bounds for $\|G(\cdot, K)\|_{L_2/L_2}$ and $\|H(X, \cdot, K) + \nabla\|_{L_2/L_2}$ explicitly? These issues will be addressed in the subsequent subsections.

Well-Definedness of $H(X, \cdot, K) + \nabla$ and Upper Bound for $\|H(X, \cdot, K) + \nabla\|_{L2/L2}$

To understand the following deductions, I_i is utilized to denote the union of all the time intervals when $y \in D_i$. By the definition of I_i, we have

$$\begin{cases} I_i \cap I_k = \varnothing, \forall i \ne k \\ \bigcup_i I_i = [0, \infty) \end{cases}$$

Note that each $\hat{H}(x_i, \delta_i, K_i) + \nabla_i$, a scalar constant, is followed by the definition that

$$\begin{aligned}
&\|H(X, \cdot, K) + \nabla\|_{L_2/L_2} \\
&= \sup_{\forall \|y\|_{L_2} \le 1} \|[H(X, y, K) + \nabla]y\|_{L_2} / \|y\|_{L_2} \\
&= \sup_{\forall \|y\|_{L_2} \le 1} [\int_0^\infty |[H(X, y(\tau), K) + \nabla]y(\tau)|^2 d\tau]^{1/2} / \|y\|_{L_2} \\
&= \sup_{\forall \|y\|_{L_2} \le 1} [\int_{\bigcup_i I_i} |[H(X, y(\tau), K) + \nabla]y(\tau)|^2 d\tau]^{1/2} / \|y\|_{L_2} \\
&= \sup_{\forall \|y\|_{L_2} \le 1} [\sum_i \int_{I_i} |[H(X, y(\tau), K) + \nabla]y(\tau)|^2 d\tau]^{1/2} / \|y\|_{L_2} \\
&= \sup_{\forall \|y\|_{L_2} \le 1} [\sum_i \int_{I_i} |\hat{H}(x_i, \delta_i, K_i) + \nabla_i|^2 |y(\tau)|^2 d\tau]^{1/2} / \|y\|_{L_2} \\
&= \sup_{\forall \|y\|_{L_2} \le 1} [\sum_i |\hat{H}(x_i, \delta_i, K_i) + \nabla_i|^2 \int_{I_i} |y(\tau)|^2 d\tau]^{1/2} / \|y\|_{L_2} \\
&\le \sup_{\forall \|y\|_{L_2} \le 1} [\max_i \{\sup_{\forall \nabla_i} |\hat{H}(x_i, \delta_i, K_i) + \nabla_i|^2\} \sum_i \int_{I_i} |y(\tau)|^2 d\tau]^{1/2} / \|y\|_{L_2} \\
&= \sup_{\forall \|y\|_{L_2} \le 1} [\max_i \{\sup_{\forall \nabla_i} |\hat{H}(x_i, \delta_i, K_i) + \nabla_i|^2\} \int_{\bigcup_i I_i} |y(\tau)|^2 d\tau]^{1/2} / \|y\|_{L_2} \qquad (9) \\
&= \max_i \{\sup_{\forall \nabla_i} |\hat{H}(x_i, \delta_i, K_i) + \nabla_i|\} \sup_{\forall \|y\|_{L_2} \le 1} [\int_0^\infty |y(\tau)|^2 d\tau]^{1/2} / \|y\|_{L_2} \\
&= \max_i \{\sup_{\forall \nabla_i} |\hat{H}(x_i, \delta_i, K_i) + \nabla_i|\}
\end{aligned}$$

where $\int_{I_i}(\cdot)(\tau)d\tau$ denotes the integral of the integrand $(\cdot)(\tau)$ over I_i. Noted by (7) that

$$\begin{aligned}
&\max_i\{\sup_{\forall\nabla_i}\left|\hat{H}(x_i,\delta_i.K_i)+\nabla_i\right|\}\\
&\le \max_i\{\left|\hat{H}(x_i,\delta_i.K_i)\right|+\sup_{\forall\nabla_i}\left|\nabla_i\right|\}\\
&=\max_i\{\left|\hat{H}(x_i,\delta_i.K_i)+\nabla_i\right|+\sup_{\forall\delta\in D_i}\left|\nabla_i\right|\}\\
&\le \max_i\{\left|\hat{H}(x_i,\delta_i.K_i)\right|\}+c<\infty
\end{aligned}$$

This, together with (9), reports that when we view $H(X,\cdot,K)+\nabla$ as a mapping from L_2 to L_2, then it is bounded; in view of this fact, it is noted that $H(X,\cdot,K)+\nabla$ is well-defined.

Well-Definedness of $G(\cdot,K)$ and Upper Bound for $\|G(\cdot,K)\|_{L_2/L_2}$

To verify our statements, we define the following time-domain projection operators.

$$P_i(t)=\begin{cases}1, & t\in I_i\\ 0, & t\notin I_i\end{cases}$$

By the definition, the following facts can be claimed.

- $\sum_i P_i \equiv 1$, $P_iP_i=P_i$, and $P_iP_k=0$ whenever $i\neq k$;
- P_iy stands for the pieces of $y(=\delta)$ that belong to D_i, while P_ie reflects those pieces of e defined on the time interval I_i;
- $G(\cdot,K)(P_iz)=\hat{G}(\cdot,K_i)(P_iz)$, where $\hat{G}(\cdot,K_i)$ stands for the LTI system whose transfer function is $\hat{G}(s,K_i)$ as explicated in (5).

From Figure 5, the time-domain relationship between e and y is

$$y(t)=G(\cdot,K)(e)(t) \tag{10}$$

In fact, $G(\cdot,K)$ represents a set of linear time-invariant differential equations that switch from one to another at isolated time points that form a set of measure zero; namely, $G(\cdot,K)$ can be interpreted as a piecewise LTI system, or equivalently it can be said that $G(\cdot,K)$ is linear almost everywhere in time ($a.e.\ t\in[0,\infty)$). The differential equation theory [O'regan] reveals that such switchings have no affect on the dynamics of $G(\cdot,K)$ on a whole. This, together with the properties of the projection operators and (10), implies that

$$\begin{aligned}
y(t)&=G(\cdot,K)(e)(t)=G(\cdot,K)(\textstyle\sum_k P_ke)(t)\\
&=\textstyle\sum_k G(\cdot,K)(P_ke)(t), \quad a.e. t\in[0,\infty)\\
&=\textstyle\sum_k \hat{G}(\cdot,K)(P_ke)(t), \quad a.e. t\in[0,\infty)
\end{aligned}$$

Now it is observed that

$$\begin{aligned}
&\|G(\cdot,K)\|_{L_2/L_2}=\sup_{\forall\|e\|_{L_2}\le 1}\|G(\cdot,K)(e)\|_{L_2}/\|e\|_{L_2}\\
&=\sup_{\forall\|e\|_{L_2}\le 1}[\int_0^\infty\left|\textstyle\sum_k\hat{G}(\cdot,K)(P_ke)(\tau)\right|^2d\tau]^{1/2}/\|e\|_{L_2}\\
&=\sup_{\forall\|e\|_{L_2}\le 1}[\frac{1}{2\pi}\int_{-\infty}^{\infty}(\textstyle\sum_k\hat{G}(j\varphi,K_k)E_k(j\varphi))^*\\
&\cdot\textstyle\sum_k\hat{G}(j\varphi,K_k)E_k(j\varphi)d\varphi]^{1/2}/\|e\|_{L_2}\\
&=\sup_{\forall\|e\|_{L_2}\le 1}[\frac{1}{2\pi}\int_{-\infty}^{\infty}\left|\hat{G}(j\varphi,K)^*E(j\varphi)\right|^2d\varphi]^{1/2}/\|e\|_{L_2}
\end{aligned} \tag{11}$$

where $(\cdot)^*$ means complex conjugate transposition, and

$$\hat{G}(j\varphi,K)=:\begin{bmatrix}\vdots\\ \hat{G}(j\varphi,K_{-1})\\ \hat{G}(j\varphi,K_0)\\ \hat{G}(j\varphi,K_1)\\ \vdots\end{bmatrix}\in C^N$$

$$\hat{E}(j\varphi)=:\begin{bmatrix}\vdots\\ E_{-1}(j\varphi)\\ E_0(j\varphi)\\ E_1(j\varphi)\\ \vdots\end{bmatrix}\in C^N$$

where N is the number of the sub-regions in the phase plane partitioning D. In (11), the Parseval theorem is used for the pair $\hat{G}(\cdot,K_k)(P_ie)$ and $\hat{G}(j\varphi,K_k)E_k(j\varphi)$. Here, $E_k(j\varphi)$ is the Fourier transform of P_ke. $E_k(j\varphi)$ is well-defined since $P_ke\in L_2$ for $e\in L_2$.

Applying the Cauchy-Schwarz inequality to the last equation of (11), we continue

$$\begin{aligned}
&\|G(\cdot,K)\|_{L_2/L_2} \\
&\le \sup_{\forall e_{L_2}\le 1}[\frac{1}{2\pi}\int_{-\infty}^{\infty}(\hat{G}(j\varphi,K)^*\hat{G}(j\varphi,K)) \\
&\cdot(E(j\varphi)^*E(j\varphi))d\varphi]^{1/2}/\|e\|_{L_2} \\
&= \sup_{\forall e_{L_2}\le 1}[\frac{1}{2\pi}\int_{-\infty}^{\infty}(\Sigma_k \hat{G}(j\varphi,K)^*\hat{G}(j\varphi,K)) \\
&\cdot(\Sigma_k E(j\varphi)^*E(j\varphi))d\varphi]^{1/2}/\|e\|_{L_2} \\
&\le \sup_{\forall e_{L_2}\le 1}[\frac{1}{2\pi}\int_{-\infty}^{\infty}(\Sigma_k \|\hat{G}(\cdot,K)\|_\infty^2) \\
&\cdot(\Sigma_k E(j\varphi)^*E(j\varphi))d\varphi]^{1/2}/\|e\|_{L_2} \\
&= \sqrt{\Sigma_k \|\hat{G}(\cdot,K)\|_\infty^2} \\
&\cdot \sup_{\forall e_{L_2}\le 1}[\frac{1}{2\pi}\int_{-\infty}^{\infty}\Sigma_k E(j\varphi)^*E(j\varphi))d\varphi]^{1/2}/\|e\|_{L_2} \\
&=: \|G(\cdot,K)\|_\infty \\
&\cdot \sup_{\forall e_{L_2}\le 1}[\frac{1}{2\pi}\int_{-\infty}^{\infty}(\Sigma_k E_k(j\varphi)^*)\Sigma_i E_i(j\varphi)d\varphi]^{1/2}/\|e\|_{L_2} \\
&=: \|G(\cdot,K)\|_\infty
\end{aligned} \tag{12}$$

where $\|G(\cdot,K)\|_\infty =: (\Sigma_k \|\hat{G}(\cdot,K_k)\|_\infty{}^2)^{1/2}$. In (12), we have used the following facts:

$$\begin{aligned}
&\tfrac{1}{2\pi}\int_{-\infty}^{\infty} E_k(j\varphi)^* E_i(j\varphi)d\varphi \\
&= \int_0^{\infty}(P_k e)(\tau)^*(P_i e)(\tau)d\tau = 0
\end{aligned}$$

whenever $i \neq k$; and

$$\begin{aligned}
&[\frac{1}{2\pi}\int_{-\infty}^{\infty}(\Sigma_k E_k(j\varphi))^*\Sigma_i E_i(j\varphi)d\varphi]^{1/2} \\
&= [\int_0^{\infty}(\Sigma_k P_k e(\tau))^*\Sigma_i P_k e(\tau)d\tau]^{1/2} \\
&= [\int_0^{\infty} e(\tau)^* e(\tau)d\tau]^{1/2} = \|e\|_{L_2}
\end{aligned}$$

The facts follow from the Parseval theorem and the properties of the projection operators.

Since $\|\hat{G}(\cdot,K_k)\|_\infty < \infty$ for each k and we only consider the case with finite many sub-regions, therefore we have $\|G(\cdot,K)\|_\infty < \infty$. It is revealed that when $G(\cdot,K)$ is a bounded mapping from L_2 to L_2; or equivalently, that $G(\cdot,K)$ is well-defined. The well-definedness of $G(\cdot,K)$ and that of $H(X,\cdot,K)+\nabla$ validate our arguments about the small-gain inequality (8).

Interpreting the Small-Gain Stability Criterion with (9) and (12)

With the upper bounds for $\|H(X,\cdot,K)+\nabla\|_{L_2/L_2}$ and $\|G(\cdot,K)\|_{L_2/L_2}$, namely (9) and (12), It can be concluded from the small-gain inequality (8) that for a prescribed gain-scheduling loop transformation K, if we can design a gain-scheduling control law X such that

$$\|G(\cdot,K)\|_\infty \cdot \max_i\{\sup_{\forall\nabla_i}|\hat{H}(x_i,\delta_i,K_i)+\nabla_i|\} < 1 \tag{13}$$

then the closed-loop IGS is finite-gain L_2 stable.

The small-gain inequality (13) is a sufficient condition. Examining (13) carefully, one will realize that existence and performance of the gain-scheduling control law X for maneuvering the SVC are closely related to the gain-scheduling loop transformation K. There are numerous ways to exploit the small-gain inequality (13) in determining appropriate gain-scheduling control laws in form of $X = \{\cdots, x_{-1}, x_0, x_1, \cdots\}$ for manipulating the SVC reactance.

Stabilizing the IGS with Gain-Scheduling SVC

In this section, we first discuss possible gain-scheduling control laws of the SVC when only stabilization is concerned. Then it is shown that the gain-scheduling SVC control law can also be employed for power angle specification, which is one of the most important steady-state performances for synchronous generators. Finally, it is verified that stabilization and steady-state performance specification in the IGS can be implemented simultaneously with a single gain-scheduling SVC.

Stabilization under Average Gain-Scheduling SVC Algorithm

It is clear that the small-gain inequality (13) holds as long as

$$\|G(\cdot,K)\|_\infty \cdot \|\hat{H}(x_i,\delta_i,K_i)+\nabla_i\| < 1 \tag{14}$$

for each i and for all ∇_i; that is, each x_i is determined with respect to the gain-scheduling loop transformation $K = \{\cdots, K_{-1}, K_0, K_1 \cdots\}$ such that (14) is true. More explicitly, we write

$$|\theta(\delta_i)x_i^{-1} - K_i + \nabla_i| < 1/\|G(\cdot,K)\|_\infty$$

for each i and for all ∇_i. Clearly, the above inequality can be equivalently interpreted as

$$\begin{cases} \theta(\delta_i)x_i^{-1} - K_i + \nabla_i < 1/\|G(\cdot,K)\|_\infty, \\ \quad if \quad \theta(\delta_i)x_i^{-1} \geq K_i - \nabla_i \\ -\theta(\delta_i)x_i^{-1} + K_i - \nabla_i < 1/\|G(\cdot,K)\|_\infty, \\ \quad if \quad \theta(\delta_i)x_i^{-1} < K_i - \nabla_i \end{cases}$$

for each i and for each fixed ∇_i. More simply we write

$$\begin{cases} \theta(\delta_i)x_i^{-1} < K_i - \nabla_i + 1/\|G(\cdot,K)\|_\infty, \\ \quad if \quad \theta(\delta_i)x_i^{-1} \geq K_i - \nabla_i \\ \theta(\delta_i)x_i^{-1} > K_i - \nabla_i - 1/\|G(\cdot,K)\|_\infty, \\ \quad if \quad \theta(\delta_i)x_i^{-1} < K_i - \nabla_i \end{cases} \tag{15}$$

for each i and for each fixed ∇_i. It is not hard to see that for each i and any given $K_i > 0$ and each fixed ∇_i, if we can choose x_i to satisfy both of the inequalities in (16),

$$\begin{aligned} K_i - \nabla_i - 1/\|G(\cdot,K)\|_\infty &< \theta(\delta_i)x_i^{-1} \\ &< K_i - \nabla_i + 1/\|G(\cdot,K)\|_\infty \end{aligned} \tag{16}$$

then at least one of the inequalities in (15) is true. Furthermore, it is noted that

$$\begin{aligned} & K_i - \nabla_i + 1/\|G(\cdot,K)\|_\infty - (K_i - \nabla_i - 1/\|G(\cdot,K)\|_\infty) \\ & = 2/\|G(\cdot,K)\|_\infty > 0 \end{aligned}$$

It is observed that such x_i always exists as long as $\theta(\delta_i) \neq 0$ so that (16) is satisfied. $\theta(\delta_i) \neq 0$ can be guaranteed by the selection of the left boundary of D_i so that $\sin\delta_i/\delta_i \neq 0$.

Remark 1 The gain-scheduling loop transformation K is utilized to derive the small-gain inequality (13), which yields the gain-scheduling SVC control law (16). K should be implemented nowhere in the closed-loop IGS; and the control law X satisfying (16) is only embodied. The gain-scheduling loop transformation K plays its role indirectly in the closed-loop IGS via the control law X. A different gain-scheduling loop transformation brings different effect into the closed-loop IGS. There are infinitely many possibilities to set x_i such that (16) is satisfied.

Remark 2 A simple way to parameterize the SVC reactance is to choose the average evaluation of $K_i - \nabla_i + 1/\|G(\cdot,K)\|_\infty$ and $K_i - \nabla_i + 1/\|G(\cdot,K)\|_\infty$, namely

$$\theta(\delta_i)x_i^{-1} = \left(\frac{K_i - \nabla_i - 1}{\|G(\cdot,K)\|_\infty} + \frac{K_i - \nabla_i + 1}{\|G(\cdot,K)\|_\infty}\right)/2 = K_i - \nabla_i$$

or

$$x_i^{-1} = (K_i - \nabla_i)\theta(\delta_i).$$

In this averagely gain-scheduling SVC algorithm, there is no need to compute any H_∞ norm for the involved LTI models.

One can take $K_i > 0$ sufficiently large, and at the same time let $|\nabla_i|$ sufficiently small by partitioning the phase plane in the sense of $d \to 0$, see Figure 4. Then the averagely gain-scheduling SVC algorithm reasonably and approximately reduces to

$$x_i^{-1} = K_i / \theta(\delta_i) \tag{17}$$

Our approximating $x_i^{-1} = (K_i - \nabla_i)\theta(\delta_i)$ can be validated by (17) as follows. Let us return to Figure 5 and notice that the feedback signal caused by the modeling mismatch ∇ can simply be attributed to P_Δ by separating ∇ and $H(X,\cdot,K)$ (that is, ∇y is treated as part of the power disturbance P_Δ), and then the previous arguments can be repeated similarly without taking ∇ into account. In this way, we once again led to (17) eventually. In view of this, the stabilization control law (17) is robust against modeling uncertainties and power disturbance. This is highly expected in generator stabilization engineering.

Transient and Steady-State Performances Specification

At first, we explicate how the loop transformation parameter K (or equivalently the gain-scheduling control law (17)) is used to affect transient characteristics of the closed-loop IGS.

According to Figure 3, the transfer function from $P_m + P_\Delta$ to y when the SVC reactance is set at the averagely gain-scheduling control law (17) is given by

$$\begin{aligned} \hat{G}_C(s,x_i) &= \frac{\hat{G}(s,K_i)}{1 + \hat{G}(s,K_i)\hat{H}(x_i,\delta_i,K_i)} \\ &= \frac{G(s)}{1 + G(s)\theta(\delta_i)x_i^{-1}} = \frac{G(s)}{1 + G(s)K_i} \\ &= \frac{1/M}{s^2 + (D/J)s + K_i/M} \end{aligned}$$

where the fact is employed that the loop

transformation K_i can be removed simply due to the configuration. Clearly, the poles of $\hat{G}_C(s,x_i)$ are given by

$$\lambda_{1,2} = -D/(2J) \pm \sqrt{D^2/(2J)^2 - K_i/M} \qquad (18)$$

Remark 3 Clearly, for any $K_i > 0$, $\mathrm{Re}(\lambda_{1,2}) < 0$. It is also observed that the bigger $K_i > 0$ is, the more quickly the SVC control will be affected. Bearing this in mind, we can prescribe the gain-scheduling loop transformation $K = \{\cdots, K_{-1}, K_0, K_1 \cdots\}$ as follows; if the power angle δ deviates far from the equilibrium point, then bigger $K_i > 0$ is taken so that the SVC drives the δ -dynamics more quickly back to the equilibrium; otherwise, smaller $K_i > 0$ is taken to avoid overshooting.

Secondly, steady-state performance specification is taken into consideration by means of the loop transformation parameter K (or equivalently the gain-scheduling control law (17)).

Power angle of the IGS in the steady state, $y_{ss} = \lim_{t\to\infty} y(t)$, is closely related to power generation efficiency of the concerned generator. Hence, how to adjust the SVC reactance for the closed-loop IGS to attain a desired power angle performance, say δ_{ss}, is significant. In this section, it is explicated that such SVC control laws do exist.

Again from Figure 3, the transfer function from $P_m + P_\Delta$ to y when the SVC is set at x_i is

$$\hat{G}_C(s,x_i) = \frac{1/M}{s^2 + (D/J)s + \theta(\delta_i)/(Mx_i)} \qquad (19)$$

The steady-state response of $\hat{G}_C(s,x_i)$ when $P_m + P_\Delta$ is a step signal in form of $U \cdot 1(t)$ is

$$y_{ss} = \lim_{s\to 0} s\frac{U}{s}\frac{1/M}{s^2 + (D/J)s + \theta(\delta_i)/(Mx_i)} = \frac{Ux_i}{\theta(\delta_i)}$$

Remark 4 From the above steady-state relationship, it is seen that one can specify the steady-state performance of y to the desired position $y_{ss} = \delta_{ss}$ by setting the SVC reactance x_i as follows.

$$x_i = \frac{\delta_{ss}}{U}\theta(\delta_i) \qquad (20)$$

Congruence between Stabilization and Steady-State Specification in the Same Average Gain-Scheduling SVC Algorithm

In the preceding subsections, stabilization, transient response features and steady-state performance specification for the closed-loop IGS are tackled which are governed by (17), (18) and (20), respectively. Since these three objectives are expected to be attained by a same and single SVC, such a question is inevitable: whether a gain-scheduling loop transformation K and a gain-scheduling control law X exists such that (17), (18) and (20) are satisfied simultaneously. Here only the parametrization congruence issue between (17) and (20) is in consideration.

When the IGS runs into steady state, it is assumed that the SVC control law is determined under a loop transformation $K_i = K_0$ over a sub-region $D_i = D_0$, in which the desired power angle δ_{ss} is located. Hence, the congruence issue can be formulated as follows: to achieve the steady-state performance specification $x_i = x_0$ of (20), that is,

$$x_0 = \frac{\delta_{ss}}{U}\theta(\delta_0) \qquad (21)$$

while a loop transformation $K_0 > 0$ can be fixed such that

$$\frac{K_0 - \nabla_0 - 1}{\|G(\cdot,K)\|_\infty} < \theta(\delta_0)x_0^{-1} < \frac{K_0 - \nabla_0 + 1}{\|G(\cdot,K)\|_\infty} \qquad (22)$$

where the assumption is that K_0 is sufficiently larger than ∇_0.

Now we observe by (21) that

$$\theta(\delta_0)x_0^{-1} = \theta(\delta_0)(\frac{\delta_{ss}}{U}\theta(\delta_0))^{-1} = \frac{U}{\delta_{ss}} > 0$$

Therefore, if let $K_0 = U/\delta_{ss}$, the steady-state performance specification control law (21) satisfies (22) immediately. This leads us to the desired congruence between (17) and (20).

The congruence between stabilization and steady-state performance specification indicates that the steady-state performance specification control law of the SVC automatically guarantees finite-gain L_2 -stability in the closed-loop IGS, as long as control laws over other

sub-regions run according to (17) that ensures the small-gain theorem condition (16).

Numeric Illustrations

Numeric illustrations show that the averagely gain-scheduling control laws of SVC's given in (17) is a simple and effective technique to stabilize individual generators, while steady-state features of the closed-loop IGS's can be specified. Table 1 lists the coefficients of an example IGS.

TABLE 1 COEFFICIENTS OF THE EXAMPLE INDIVIDUAL GENERATOR

b : maximum power capacity	950(kw)
D : amortisseur damping constant	95
J : combined inertia moment	550(kg.m²)
ω_s : system angular frequency	$2\pi\times 60$(rad /sec)
P_m : mechanical power	475(kw)
x_g : reactance between B_m and B_g	0.6(Ω)
x_l : reactance between B_m and B_c	0.4(Ω)

In the numeric simulation, all time response curves are plotted via the second-order Runga-Kutta algorithm [Vidyasagar] with $[\delta(0),\omega(0)]^T$ randomly given within $\delta(0)\in[-1,1]$ and $\omega(0)\in[-1,1]$, and the step length 0.01(sec). The solid lines represent the time behaviours of the generator rotor with SVC installed, while the dash-dotted lines stand for those without SVC. The disturbance P_Δ is white noise with $|P_\Delta|\le 20$ (kw).

SVC Actions Based on the Averagely Gain-Scheduling Control Law

Only the control law suggested in Remark 2 is in consideration. We partition the phase plane into equitable sub-regions as follows: the sub-region $\delta_{ss}\in D_0$ is

$$D_0=\{(\delta,\omega)\in R^2:\delta_{ss}-\Delta\delta\le\delta<\delta_{ss}+\Delta\delta\}$$

where $\Delta\delta$ means a deviation from δ_{ss} . In the following, we take $\Delta\delta=\delta_{ss}\times 10\%$.

All other sub-regions locating to the left or the right of D_0, namely D_i, are

$$D_i=\{(\delta,\omega)\in R^2:\delta_{ss}+(2i-1)\Delta\delta\le\delta<\delta_{ss}+(2i+1)\Delta\delta\}$$

where $i=\cdots,-2,-1,1,2,\cdots$. According to the phase plane partitioned, a gain-scheduling loop transformation $K=\{\cdots,K_{-1},K_0,K_1\cdots\}$ is prescribed. Taking the steady-state specification $\lim_{t\to\infty}\delta=\delta_{ss}$ into consideration, and for numeric simplicity, we will take

$$K_0=\frac{U}{\delta_{ss}}>0,\cdots K_{-2}=K_{-1}=K_1=K_2=\cdots=K_{\bar{0}}>K_0$$

Consequently, the averagely gain-scheduling algorithm of the SVC is

$$\begin{cases} x_0=\dfrac{\delta_{ss}b\sin(\delta_{ss}-\Delta\delta)}{U(\delta_{ss}-\Delta\delta)}, & \forall\delta\in D_0 \\ x_i=\dfrac{b\sin(\delta_{ss}+(2i-1)\Delta\delta)}{K_{\bar{0}}(\delta_{ss}+(2i-1)\Delta\delta)}, & \forall\delta\in D_i\,(i\ne 0) \end{cases}$$

Simulation Results and Observation

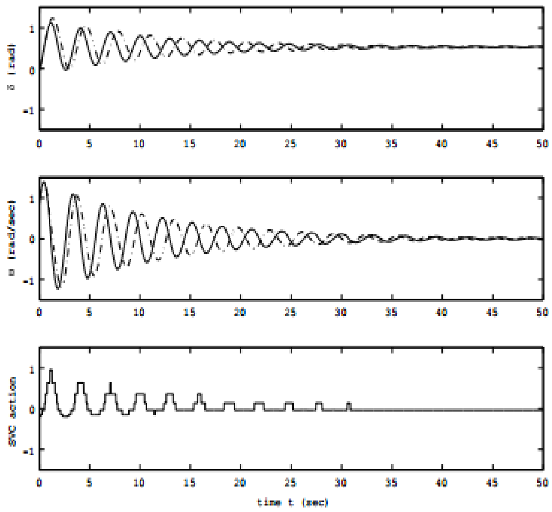

FIG. 6 TIME RESPONSE CURVES WHEN $\delta_{ss}=30^\circ$ (OR $\pi/6$ (rad))

In Figure 6, the steady-state power angle is specified at $\delta_{ss}=30^\circ$ or 0.5236 (rad), which is also the intrinsic steady-state power angle of the individual generator (that is, when the SVC is not installed). By this structural feature, it is not strange to see that the SVC is actually switched off in the steady state.

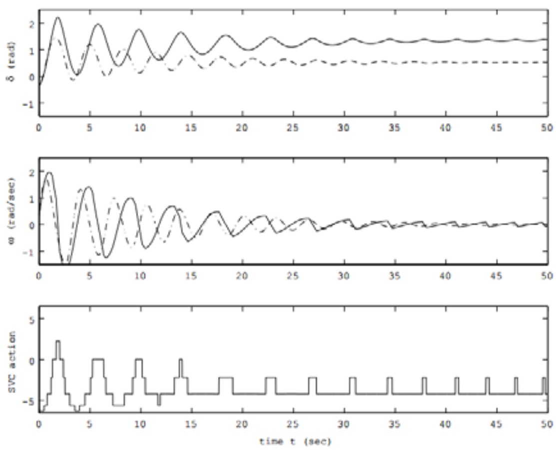

FIG. 7 TIME RESPONSES CURVES WHEN $\delta_{ss}=72^\circ$ (OR 1.2566 (rad))

In Figure 7, the steady-state power angle is specified at $\delta_{ss} = 72^{\circ}$ or 1.2566 (rad). Compared to the case of Figure 6, since the steady-state power angle is different from the intrinsic power angle, the SVC must provide manipulation affect even in the steady state.

The numeric results of Figure 8 clearly reveals that for some initial conditions, the generator rotor may run simply out of synchronism without enacting the SVC; in other words, the suggested gain-scheduling SVC control law does stabilize the IGS system, while the steady-state power angle is driven to the desired position $\delta_{ss} = 72^{\circ}$ or 1.2566 (rad).

Conclusions

Robustly stabilizing individual generators in multi-machine networks in the finite-gain L2-stability sense via output-feedback-controlled flexible ac tra nsmiss ion system devices is considered in the paper for the first time. In detail, individual generator dynamics are characterized with a linear time invariant modeling and a nonlinear feedback, with modeling uncertainties and power disturbances taken into account. Based on such modeling, control laws of SVC's are contrived to stabilize the individual generators. The control laws of SVC's are developed by exploiting the gain-scheduling framework based on the small-gain theorem. It is also shown that SVC's can be employed for power angle specification in individual generator systems.

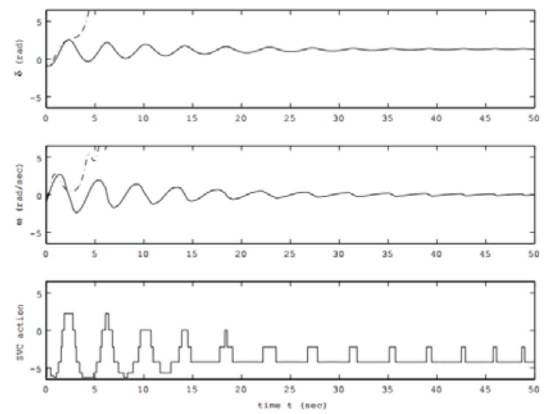

FIG. 8 TIME RESPONSES CURVES WHEN THE IGS MAY BE UNSTABLE WITHOUT SVC

The suggested stabilization approach possesses several advantages, such as, it can be implemented in various decentralized fashions that employ only local feedback; or it can cope with damping windings that are neglected in the equal area criterion technique; and it results in robust stabilization in individual generator systems subject to modeling uncertainties and power disturbances stemming from governors and loads; the SVC control laws can also adaptive to the specification requirements on steady-state power angle. It is worth mentioning that SVC control laws may also be contrived by means of artificial intelligent techniques such as fuzzy control and etc.

ACKNOWLEDGMENT

The work is supported by National Nature Science Foundation of China under Grant 61074186.

APPENDIX A: PROPERTIES RELATED TO $\|G(\cdot,K)\|_{\infty}$

In the main context, we only consider the averagely gain-scheduling SVC algorithm that has nothing to do with the numeric computation of $\|G(\cdot,K)\|_{\infty}$. However, the small-gain inequality (16) actually can have various implementation algorithms beside the suggested average one, some of which may need the computation of $\|G(\cdot,K)\|_{\infty}$. Hence it is necessary to learn more about $\|G(\cdot,K)\|_{\infty}$ to facilitate its numeric computation.

Since $\|G(\cdot,K)\|_{\infty}$ are determined by $\|\hat{G}(\cdot,K_i)\|_{\infty}$, we collect basic facts about $\|\hat{G}(\cdot,K_i)\|_{\infty}$ for a fixed i. Again noticing that $\hat{G}(\cdot,K_i)$ stands for an LTI system, whose transfer function is nothing but $\hat{G}(s,K_i)$ that is stable for any $K_i > 0$, we obtain

$$
\begin{aligned}
\|\hat{G}(\cdot,K_i)\|_{\infty} &= \sup_{\varphi\in(-\infty,\infty)} |\hat{G}(j\varphi,K_i)| \\
&= \sup_{\varphi\in(-\infty,\infty)} \{(K_i - M\varphi^2)^2 + (MD/J)^2\varphi^2\}^{-1/2} \\
&= \{\inf_{\varphi\in(-\infty,\infty)} F(\varphi,K_i)\}^{-1/2}
\end{aligned}
\tag{23}
$$

where $F(\varphi,K_i) = (K_i - M\varphi^2)^2 + (MD/J)^2\varphi^2$.

Taking the derivative on $F(j\varphi,K_i)$ with respect to φ, we obtain

$$dF(\varphi,K_i)/d\varphi = -4M\varphi(K_i - M\varphi^2) + 2(MD/J)^2\varphi$$

which indicates that lower bounds of $F(j\varphi,K_i)$ may appear at

$$
\begin{cases}
\varphi_1 = 0, \\
\qquad 0 < K_i \le M(D/J)^2/2 \\
\varphi_1 = 0, \varphi_{2,3} = \pm\sqrt{K_i/M - (D/J)^2/2}, \\
\qquad K_i > M(D/J)^2/2
\end{cases}
\tag{24}
$$

Based on (23) and (24), we can conclude:

- If $0 < K_i \le M(D/J)^2/2$, $\inf F(\varphi, K_i)$ is attained only at φ_1 so that

$$\left\|\hat{G}(\cdot, K_i)\right\|_\infty = 1/K_i \tag{25}$$

- If $K_i > M(D/J)^2/2$, $\inf F(\varphi, K_i)$ is attained at φ_1, φ_2 and φ_3 so that

$$\begin{aligned}&\left\|\hat{G}(\cdot, K_i)\right\|_\infty \\ &= \max\{\left|\hat{G}(j\varphi_1, K_i)\right|, \left|\hat{G}(j\varphi_2, K_i)\right|, \left|\hat{G}(j\varphi_3, K_i)\right|\}\end{aligned}$$

We have already known that $\left|\hat{G}(j\varphi_1, K_i)\right| = 1/K_i$. Furthermore, we observe

$$\begin{aligned}&\left|\hat{G}(j\varphi_2, K_i)\right| = \left|\hat{G}(j\varphi_3, K_i)\right| \\ &= \{(K_i - M[2K_i - M(D/J)^2]/(2M))^2 \\ &+ (MD/J)^2[2K_i - M(D/J)^2]/(2M)\}^{-1/2} \\ &= \{(K_i - [K_i - M(D/J)^2/2])^2 \\ &+ M(D/J)^2[K_i - M(D/J)^2/2]\}^{-1/2} \\ &= \{(M(D/J)^2/2)^2 + M(D/J)^2 K_i \\ &- M^2(D/J)^4/2\}^{-1/2} \\ &= \{M(D/J)^2 K_i - M^2(D/J)^4/4\}^{-1/2} > 1/K_i\end{aligned}$$

The last inequality follows from $K_i > M(D/J)^2/2^2$.

In summary, it is concluded that the larger $K_i > 0$ is, the smaller $\left\|\hat{G}(\cdot, K_i)\right\|_\infty$ is, and

$$\begin{cases} 0 < K_i \le M(D/J)^2/2, \\ \qquad \left\|\hat{G}(\cdot, K_i)\right\|_\infty = 1/K_i \\ K_i > M(D/J)^2/2, \\ \qquad \left\|\hat{G}(\cdot, K_i)\right\|_\infty = \\ \qquad \{M(D/J)^2 K_i - M^2(D/J)^4/4\}^{-1/2} > 1/K_i \end{cases}$$

REFERENCES

C. W. Liu, J. S. Thorp, J. Lu, R. J. Thomas and H. D. Chiang, Detection of transiently chaotic swings in power-systems using real-time phasor measurements, IEEE Transactions on Power Systems, vol. 9, no. 3, pp. 1285-1292, 1994.

D. O'Regan, Existence Theory for Nonlinear Ordinary Differential Equations, Kluwer Academic Publishers, 1997.

E. Lerch, D. Povh and L. Xu, Advanced SVC control for damping power system oscillations, IEEE Transactions on Power Systems, vol. 60, no. 2, pp. 524-531, 1991.

E. W. Kimbark, Power System Stability, Vol. I, , 1995.

E. Z. Zhou, Application of static VAR compensators to increase power system damping, IEEE Transactions on Power Systems, vol. 8, no. 2, pp. 655-661, 1993.

F. M. A. Salam, Asymptotic stability and estimating the region of attraction for the swing equations, Systems & Control Letters, vol. 7, no. 4, pp. 309-312, 1986.

G. Damm, R. Marino and F. Lamnabhi-Lagarrigue, Adaptive nonlinear output feedback for transient stabilization and voltage regulation of power generators with unknown parameters,International Journal of Robust and Nonlinear Control, vol. 14, pp. 833-855, 2004.

H. D. Chiang and C. C. Chu, Stability regions of nonlinear autonomous dynamical systems, IEEE Transactions on Automatic Control, vol. 33, no. 1, pp. 16-17, 1988.

H. K. Khalil, Nonlinear Systems, 3rd Ed., Prentice Hall, 2002.

J. Machowski, J. W. Bialek and J. R. Bumby, Power system dynamics and stability, John Wiley & Sons, New York, 1997.

J. Zhou and Y. Ohsawa, Improved swing equation and its properties in synchronous generators, IEEE Transactions on Circuits and Systems-I: Regular Papers, vol. 56, no. 1, pp. 200-209, 2009. DOI: 10.1109/TCSI.2008.924895.

J. Zhou, Individual generator modeling in multi-machine networks and its stabilization with SVC, IEEJ Transactions on Electrical and Electronic Engineering, vol. 5, no. 2, pp. 229-236, 2010. DOI version: http://dx.doi.org/10.1002/tee.20521.

J. Zhou, Stabilization of individual generators with SVC designed via phase plane partitioning, IET Control Theory and Applications, vol. 4, no. 4, pp. 601-612, 2010. DOI: 10.1049/ietcta.2009.0069.

K. Zhou and J. C. Doyle, Essentials of Robust Control, Prentice Hall, 1998.

L. Cong, Y. Wang and D. J. Hill, Co-ordinated control design of generator excitation and SVC for transient stability and voltage regulation enhancement of multi-machine power systems, International Journal of Robust and Nonlinear Control, vol. 14, pp. 789-805, 2004.

L. F. C. Alberto and N. G. Bretas, Synchronism versus stability in power systems, International Journal of Electrical Power & Energy Systems, vol 21, no. 4, pp. 261-267, 1999.

L. L. Fan and A. Feliachi, Decentralized stabilization of nonlinear electric power systems using local measurements and feedback linearization, Proceedings of the 43rd IEEE Mideast Symposium on Circuits and systems, vol. 2. pp. 638- 641, 2000.

M. E. Aboul-Ela, A. A. Sallam, J. D. McCalley and A. A. Fouad, Damping controller design for power system oscillations using global signals, IEEE Transactions on Power Systems, vol. 11, no. 2, pp. 767-773, 1996.

M. H. Haque, Application of energy function to assess the first-swing stability of a power system with an SVC, IEE Proc.-Gener. Transm. Distrib., vol. 152, no. 6, pp. 806-812, 2005.

M. H. Haque, Improvement of first swing stability limit by utilizing full benefit of shunt FACTS devices, IEEE Transactions on Power Systems, vol. 19, no. 4. pp. 1894-1902, 2004.

M. Vidyasagar, Nonlinear Systems Analysis, 2nd ed., Prentice-Hall, Inc., Cliffs, NJ, 2002.

P. M. Anderson and A. A. Fouad, Power System Control and Stability, 2nd Ed, 2003.

Q. Lu, S. W. Mei, F. F. Wu, Y. X. Ni and T. L. Shen, Nonlinear decentralized disturbance attenuation excitation control via new recursive design for multi-machine power systems, IEEE Transactions on Power Systems, vol. 16, no. 4, pp. 729-736, 2001.

R. Gupta, B. Bandyopadhyay and A. M. Kulkarni, Power system stabilizer for multi-machine power system using robust decentralised periodic output feedback, IEE Proceedings of Control Theory and Applications, vol. 152, no. 1, pp. 3-8, 2005.

T. C. Yang, N. Munro and A. Brameller, A new decentralized stabilization method with application to power system stabilizer design for multi-machine systems. International Journal of Electrical Power & Energy Systems, vol. 9, pp. 206-261, 1987.

T. C. Yang, Synchronous generator stabilizer design through incomplete state feedback, International Journal of Electrical Power & Energy Systems, vol 16, no. 2, pp. 91-95, 1994.

Y. Y. Wang, D. J. Hill, and G. X. Guo, Robust decentralized control for multi-machine power systems, IEEE Transactions on Circuits and Systems-I, vol. 45, no. 3, pp. 271-279, 1998.